Original paper

Folia Neuropathologica

The effect of chemotherapies on the crosstalk interaction between CD8 cytotoxic T-cells and MHC-I peptides in the microenvironment of WHO grade 4 astrocytoma

Nadeem Butt[1], Maryam Enani[2], Maryam Alshanqiti[3], Alaa Alkhotani[4], Taghreed Alsinani[5], Mohammed Matoog Karami[6], Motaz M Fadul[1], Majid Almansouri[7], Amber Hassan[8], Saleh Baeesa[9], Ahmed K Bamaga[10], Shadi Alkhayyat[11], Eyad Faizo[12], Maher Kurdi[1]

[1]Department of Pathology, Faculty of Medicine, King Abdulaziz University, Rabigh, Saudi Arabia, [2]Department of Surgery, King Abdulaziz University Hospital, Jeddah, Saudi Arabia, [3]Department of Neurosurgery, King Fahad General Hospital, Madinah, Saudi Arabia, [4]Department of Pathology, College of Medicine, Umm Al-Qura University, Mecca, Saudi Arabia, [5]Department of Neurosurgery, King Fahad General Hospital, Jeddah, Saudi Arabia, [6]Department of Clinical Physiology, Faculty of Medicine, King Abdulaziz University, Jeddah, Saudi Arabia, [7]Department of Clinical Biochemistry, Faculty of Medicine, King Abdulaziz University, Jeddah, Saudi Arabia, [8]Department of Laboratory of Translation Neuroscience, CEINGE, Biotecnologie Avanzate, Naples, Italy, [9]Department of Neuroscience, King Faisal Specialist Hospital and Research Center, Jeddah, Saudi Arabia, [10]Department of Pediatrics, King Abdulaziz University and Hospital, Jeddah, Saudi Arabia, [11]Department of Internal Medicine, Faculty of Medicine, King Abdulaziz University, Jeddah, Saudi Arabia, [12]Department of Surgery, Faculty of Medicine, University of Tabuk, Tabuk, Saudi Arabia

Folia Neuropathol 2023; 61 (3): 317-325 *DOI: https://doi.org/10.5114/fn.2023.131014*

Abstract

Introduction: *CD8⁺ T-cells and MHC-I have been detected in brain gliomas with a significant outcome. The effect of chemotherapies on the crosstalk interaction between CD8⁺ T-cells and MHC-I has never been explored.*

Material and methods: *The protein expression profiling of CD8 cytotoxic T-cells and the gene expression assay of MHC-I in 35 patients diagnosed with WHO grade 4 astrocytoma were performed. The impact of these two factors on tumor recurrence was analyzed.*

Results: *IDH was wildtype in 13 tumors. MHC-I protein expression was absent or low in 34 tumors and dense in a single case. MHC-I gene expression was upregulated in 10 tumors and 25 tumors showed MHC-I gene downregulation. Temozolomide (TMZ) was given to 24 patients and 11 patients received TMZ plus other chemotherapies. No statistically significant association was observed between IDH mutation and CD8⁺ T-cells (p = 0.383). However, this association was significant in recurrence-free interval (RFI) (p = 0.012). IDH-wildtype tumors with highly infiltrated CD8⁺ T-cells or IDH-mutant tumors with low CD8⁺ T-cells showed late tumor recurrence. There was a statistically significant difference in RFI between tumors with different MHC-I expression and CD8⁺ T-cell counts after treatment with TMZ or TMZ plus (p = 0.026).*

Conclusions: *No association between IDH mutation and CD8⁺ cytotoxic T-cell was found. IDH is directly linked to tumor recurrence regardless of CD8⁺ T-cells infiltration. TMZ plus other adjuvants is proved to be more effective in improving patient survival and delaying tumor recurrence, as compared to using TMZ alone. Nonetheless, none-TMZ adjuvants may increase tumor sensitization to cytotoxic T-cells more than TMZ.*

Key words: *WHO grade 4 astrocytoma, MHC-I, CD8, chemotherapies, recurrence.*

Communicating author:

Maher Kurdi, MD, FRCPC, FRCPath, EFN, Clinical Associate Professor of Neuropathology Department of Pathology, Faculty of Medicine, King Abdulaziz University, Rabigh, Kingdom of Saudi Arabia, e-mail: Ahkurdi@kau.edu.sa

Introduction

World Health Organization (WHO) grade 4 astrocytoma has been recently subclassified into IDH-mutant and IDH-wildtype categories. IDH-wildtype astrocytoma has been recognized as a glioblastoma. The progression of the disease is influenced by several factors such as patient age, extent of resection, and IDH mutational status, all of which have been demonstrated to affect the outcome [12]. The interaction between IDH mutation and other types of cells in the tumor microenvironment is rarely investigated. The tumor microenvironment is considered as an essential area for targeted therapies as it involves a heterogenic interaction between different cellular lineages. This interaction is dominated by neoplastic cells and immune cells [19]. Tumor associated macrophages (TAMs) and tumor infiltrating lymphocytes (TILs) are considered to be the main infiltrating immune cells in the brain tumor microenvironment [3]. TILs represent an essential component of glioma that significantly affects patient outcome [7]. These cells may be critically involved in tumor growth and progression. Intratumoral $CD8^+$ T cells exhibit a highly variable transcriptional and functional phenotypes [4,20,23]. They represent critical components of the tumor-specific adaptive immunity that attacks tumor cells [13]. The mechanism of interaction between tumor cells and TILs, mainly cytotoxic T-cells, is controlled by MHC class I (MHC-I) presentation.

MHC-I molecules play a crucial role in the immune response to glioma. These molecules are expressed on the surface of the tumor cells and provide tumor-specific peptides to cytotoxic T-cells, allowing them to identify and destroy the tumor cells [4] (Fig. 1). Upon antigen recognition, $CD8^+$ T cells undergo rapid chromatin remodeling, resulting in T-cell dysfunction [16,17,26]. Occasionally, this mechanism may be disrupted by TAMs. TAMs can surround tumor cells, hindering their identification by cytotoxic T-cells, leading to reduced T-cell activation [10,14,23]. Tumor cells can also evade the immune system by downregulating MHC-I peptides, enabling them to escape destruction by T-cells. Both mechanisms used by tumor cells to evade immunosurveillance are not yet clear, and several theories have been proposed to comprehend this process. Studies examining the association of T-cell infiltration and WHO grade 4 astrocytoma prognosis have contradictory findings, with some studies supporting an association between T cell density and survival and others not [4,5,9].

Activated TILs are known to be critical in controlling tumor progression [6,11,21]. This activation can lead

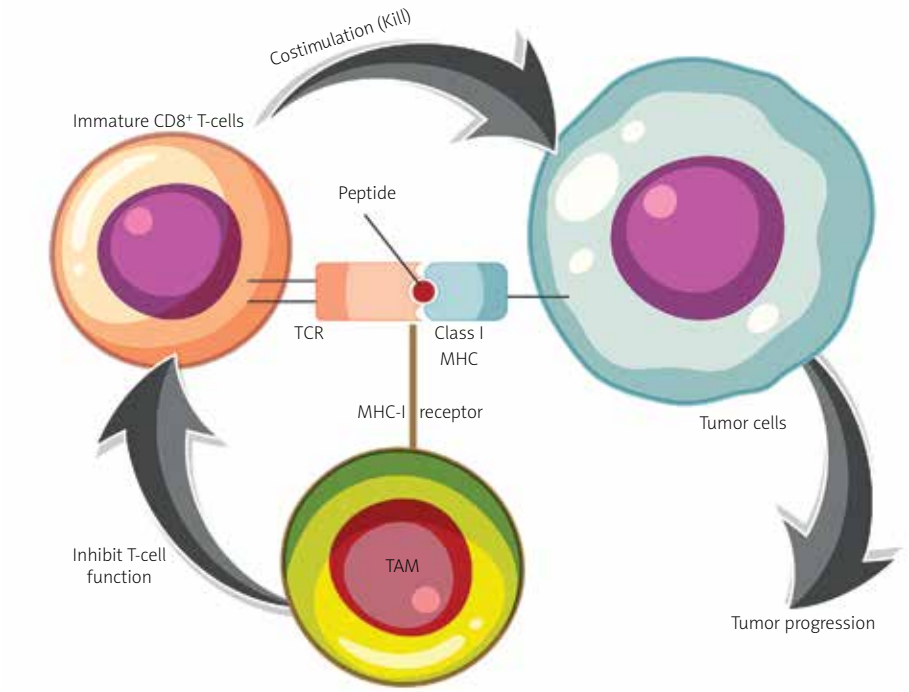

Fig. 1. Schematic diagram illustrating the crosstalk mechanism of interaction between $CD8^+$ T-cell and MHC-I on a tumor cell. The tumor cell presents MHC-I peptide on its surface to be identified and destroyed by $CD8^+$ T-cells. $CD8^+$ T-cells can be inhibited by TAMs and TAMS can also encircle tumor cells to prevent them being identified by T-cells, which cause T-cell dysfunction.

to the production of effector cytokines, including interferon (IFN) from Th1 lineage T-cells [1]. Th17 cells that express IFN can have a tumor-killing effect, whereas those that express the immune suppressive cytokine IL-10 promote tumor growth [15]. Because MHC-I antigen presentation is considered a key target where CD8 cytotoxic T-cells bind, the absence of this interaction would lead to less T-cell infiltration in the tumor microenvironment. Thus, MHC-I loss or downregulation may cause a less effective immunotherapy response. Castro *et al.* analyzed 10 glioblastoma tissues stained with MHC-I and observed that MHC-I loss is a common occurrence among patients with glioblastoma. This loss may be a major contributor to the failure of immunotherapy [2]. The loss of MHC-I expression due to mutation or deletion is frequently acquired during immunotherapy. However, this molecular alteration affecting antigen presentation may be present prior to treatment. On the other hand, high levels of $CD8^+$ T-cells bound to MHC-I antigen receptors may cause additional destruction of tumor cells. The effect of temozolomide (TMZ) therapy, with or without additional chemotherapeutic agents, in this mechanism of interaction has never been described before.

Our study aimed to investigate the dual effect of $CD8^+$ T-cell infiltration and MHC-I presentation on the progression of WHO grade 4 astrocytoma. We also examined the effect of different chemotherapeutic agents on this mechanism.

Material and methods

The study was conducted according to the guidelines of the Declaration of Helsinki and was approved by a combined Biomedical Ethics Committee between KFSH-RC and King Abdulaziz University under reference no. CA-2020-06.

Study population

We reviewed the clinical records and histological diagnoses corresponding to 35 tumors diagnosed with WHO grade 4 astrocytoma in the period 2014-2020. All patients underwent complete surgical resection followed by radiotherapy and chemotherapies. The total dosage of radiation was 60 Gy, accompanied with a standard course of TMZ [22]. Other chemotherapeutic agents such as chloroethylating agent (lomustine), procarbazine and bevacizumab were additionally given to some patients. The Ethical Committee at KFSH-RC and King Abdulaziz University [CA-2020-06] has approved the usage of patient samples in this study. Clinical and biological data of all patients enrolled in this study are retrieved and summarized in Table I. A 4 µm section of each paraffin-embedded block was utilized for protein expression measurement of anti-CD8 and MHC-I. Tissue-extracted RNA was used for MHC-I gene expression profiling using real time-polymerase chain reaction (qRT-PCR).

Protein expression measurement

Anti-MHC-I (HLA) antibody (mouse monoclonal, Abcam, clone [W6/32] Cat# of Ab22432) was utilized in the immunohistochemistry (IHC). The assay was performed on an automated stainer (Ventana, Tucson, US) using an Ultra-View detection kit. The procedure consisted of deparaffinization using EZ Prep at 75°C, heat pre-treatment with cellular medium for one hour, and incubation of 20 minutes at 37°C. The dilution was adjusted to be 1 : 400. Skeletal muscle tissue was the positive control. Anti-MHC-I stains the cytoplasmic membrane bound tumor cells. Each tissue section was examined at low magnification (10×) using light microscopy and a focal non-necrotic area with anti-MHC-I expression was selected to be examined at a higher magnification field (25×). Cells expressing MHC-I were considered as MHC-I positive. In each selected area, the labelling index (LI) of MHC-1 expression was assessed through the following equation:

$$\text{Labelling Index (\%)} = [(\text{MHC-I}^+ \text{ TC})/(\text{Total cells}) \times 100].$$

This protocol corresponds to the protocol used by Castro *et al*. presented by the American Society of Clinical Oncology Journal [2]. Three staining patterns were defined: Absent: 0% expression; Fair: < 50% expression; Dense: > 50% expression (Fig. 2). Absent and fair expression were considered as "low expression", and dense expression was considered as "high expression".

Gene expression profiling using RT-PCR

RNA was extracted from 35 tumor samples and two controls. The extraction used the RNeasy FFPE Kit (QIAGEN 73504) according to the manufacturer's protocol. All centrifugation steps were performed at 8,000 g for 15 seconds at room temperature. Each paraffin-embedded block was deparaffinized after vertexing with 1 ml of 99% m-Xylene (Sigma-Aldrich 18556). Samples were centrifuged at 17,000 g for 2 minutes to pellet the samples. The pellet was then washed with 1 ml of ethanol (100%) and centrifuged for 2 minutes. The ethanol was dried off the samples in a 37°C dry bath for 10 minutes. 150 µl of Buffer PKD was mixed thoroughly with the pellet and followed with 10 µl of Proteinase K. Samples were incubated at 56°C for 15 minutes followed by incubation at 80°C for 15 minutes. The tubes were centrifuged to pellet insoluble tissue debris and the supernatant was transferred to a clean, RNase-free 1.5 ml tube. The supernatant was

Table I. Biological data of the 35 patients with WHO grade 4 astrocytoma

Age	Gender	IDH status	MHC expression	MHC-I gene	$CD8^+$ T-cells	CTX	RFI
24	Female	IDH-mutant	Absent	Downregulated	Low expression	TMZ	600
21	Male	IDH-mutant	Absent	Downregulated	High expression	TMZ +	534
25	Male	IDH-mutant	Absent	Downregulated	High expression	TMZ +	960
29	Female	IDH-mutant	Faint	Downregulated	Low expression	TMZ	191
29	Male	IDH-mutant	Absent	Downregulated	Low expression	TMZ +	1217
31	Female	IDH-mutant	Absent	Downregulated	Low expression	TMZ	747
31	Male	IDH-mutant	Absent	Downregulated	Low expression	TMZ	680
31	Male	IDH-mutant	Absent	Downregulated	Low expression	TMZ	359
40	Male	IDH-mutant	Absent	Downregulated	Low expression	TMZ	550
43	Female	IDH-wildtype	Absent	Downregulated	High expression	TMZ +	630
44	Male	IDH-mutant	Absent	Downregulated	Low expression	TMZ	350
48	Male	IDH-wildtype	Absent	Downregulated	Low expression	TMZ	190
50	Female	IDH-wildtype	Absent	Downregulated	High expression	TMZ +	1211
51	Male	IDH-wildtype	Absent	Downregulated	Low expression	TMZ	339
51	Male	IDH-wildtype	Faint	Downregulated	High expression	TMZ	623
54	Male	IDH-wildtype	Absent	Downregulated	Low expression	TMZ	485
55	Female	IDH-wildtype	Absent	Downregulated	Low expression	TMZ	80
56	Male	IDH-mutant	Faint	Downregulated	Low expression	TMZ	130
56	Female	IDH-wildtype	Absent	Downregulated	Low expression	TMZ +	290
59	Male	IDH-mutant	Absent	Downregulated	Low expression	TMZ	229
60	Male	IDH-mutant	Absent	Downregulated	Low expression	TMZ	461
64	Male	IDH-mutant	Absent	Downregulated	Low expression	TMZ +	723
66	Female	IDH-mutant	Absent	Downregulated	Low expression	TMZ	208
67	Female	IDH-wildtype	Absent	Downregulated	Low expression	TMZ	455
25	Female	IDH-mutant	Absent	Downregulated	Low expression	TMZ +	198
45	Male	IDH-mutant	Absent	Upregulated	Low expression	TMZ	293
47	Male	IDH-mutant	Absent	Upregulated	Low expression	TMZ	566
51	Male	IDH-wildtype	Absent	Upregulated	Low expression	TMZ	128
59	Female	IDH-mutant	Absent	Upregulated	Low expression	TMZ	762
59	Male	IDH-wildtype	Faint	Upregulated	Low expression	TMZ	548
64	Female	IDH-wildtype	Absent	Upregulated	Low expression	TMZ +	490
78	Male	IDH-mutant	Absent	Upregulated	Low expression	TMZ	210
80	Male	IDH-mutant	Absent	Upregulated	Low expression	TMZ	433
83	Male	IDH-wildtype	Absent	Upregulated	High expression	TMZ +	990
85	Male	IDH-mutant	Dense	Upregulated	High expression	TMZ +	710

IDH – isocitrate dehydrogenase, MHC-I – major histocompatibility complex-1, CTX – chemotherapy, RFI – recurrence free-interval

mixed with 16 µl of DNase Buffer followed by 10 µl of DNase; the DNase was mixed gently by pipetting and left to incubate for 15 minutes. 320 µl of Buffer RBC was vortexed with the sample and 720 µl or 500 µl of ethanol was mixed by pipetting. The lysate-ethanol mixture was transferred to a spin column and centrifuged. The remaining lysate-ethanol mixture was added to the spin column, centrifuged, and the flow-through was discarded. The 500 µl of Buffer RPE was also added to the spin column, centrifuged, and the flow-through was discarded. Washing with Buffer RPE was repeated, then a new collection tube was centrifuged empty at 17,000 for 5 minutes. 1 µl of the sample was used from the RNA-containing eluates for spectrophotometric analysis. The rest of the eluate (~19 µl) was stored immediately at –20°C. The High-Capacity cDNA Reverse Transcription Kit from Applied Biosystems, 4368814, was utilized to synthesize cDNA. Briefly, a master mix was prepared with 1 µl of RT Buffer, 0.4 µl of dNTP Mix (100 mM), 1 µl of RT Random Primers, and

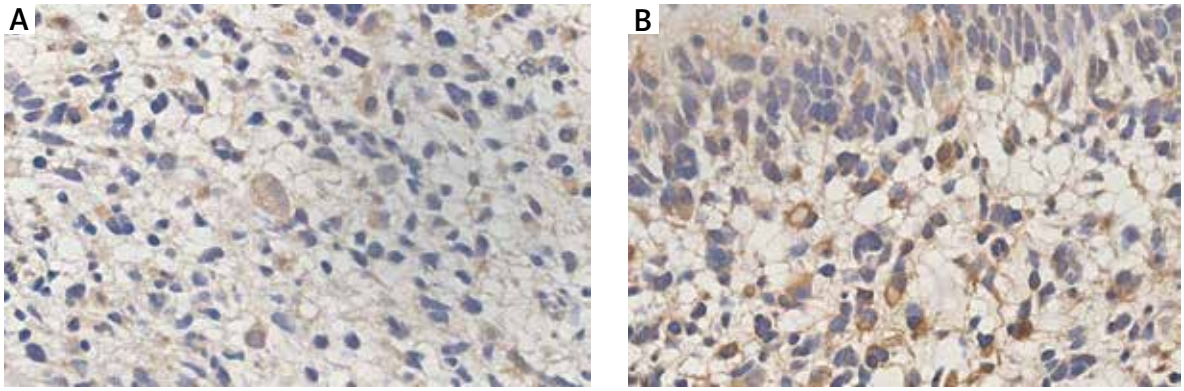

Fig. 2. MHC-I protein expression in tumor cells using IHC. **A**) Low expression, **B**) dense expression. Magnification 25×.

1 µl of MultiScribe Reverse Transcriptase was mixed with 70 ng of RNA, and the final volume was adjusted to 10 µl with RNase-free water. For samples whose concentration was < 10 ng/µl, the maximum volume of RNA was added (7.1 µl). After cDNA synthesis, 170 µl of RNase-free water was added.

The PCR primers for the experimental targeting gene (MHC-I) and the reference gene, glyceraldehyde-3-phosphate dehydrogenase (GAPDH), were pre-designed (PCR-CDA-HSA-HLAB-11). The following primer sequence for MHC-I was used in the sequencing:

Primer	Sequence	Amplicon size
Forward	5′-CCTGAGATGGGAGCCGTC-3′	89
Reverse	5′-CTCCGATGACCACAACTGCTA-3′	89

Real-time PCR was performed using the EverGreen Universal qPCR Master Mix (Haven Scientific, PCR5505), according to the manufacturer's protocol. Briefly, 4.9 µl of the resulting cDNA was mixed with 5 µl of the EverGreen master mix and the appropriate volume of each oligo for the final PCR reaction and final reaction volumes was 0.2 ml in the qPCR 96-Well Plate, Semi-Skirted plates from Haven Scientific (PCR-SSP-02). Plates were sealed with the Optical Adhesive Seal. The plates were processed on the QuantStudio3 system using a specific protocol including three minutes at 95°C, 40 cycles of 95°C for 15 seconds and finally 60°C for 60 seconds. The analysis involved two replicates of threshold cycle (C_T) values for both the target (MHC-I) and reference gene (GAPDH). Mean C_T and standard deviation were determined for both genes from the outcome data of RT-PCR. $\Delta\Delta C_T$ and ΔC_T methods were employed for analysis. The average C_T for both genes was computed from the generated data using Data Assist software. Following this, the C_T value of the target gene was adjusted to the C_T value of the reference gene. The ΔC_T of the test sample was then matched to the ΔC_T of the control sample. Using these data, the relative quantification (Rq) and fold change (FC) for differential expression were determined. ΔC_T for the control or test sample was calculated by determining the difference between the C_T value of the target gene and the C_T value of the reference gene. ΔC_T was calculated by taking the difference between the ΔC_T of the test sample and that of the control sample. Rq was determined by taking 2 raised to the power of $\Delta\Delta C_T$. ΔC_T values for each sample were determined using: ΔC_T = mean C_T reference gene – mean C_T target gene. The gene expression results are summarized in Table I.

Statistical analysis

The association between IDH mutation, CD8+ T-cells and MHC-I expression was analyzed using Fisher's exact test. The Kaplan-Meier curve (KMC) and log-rank test were used to compare the distribution of recurrence-free interval (RFI) with MHC-I expression, CD8+ T-cells, and chemotherapy type. RFI is defined as the period from post-surgical resection to the first day of tumor recurrence. A *p*-value of < 0.05 was considered statistically significant. All statistical analyses in this study were performed using IBM SPSS ver. 24.

Results

The mean patients' age was 49 years. IDH was wild-type in 13 tumors (37%). MHC-I protein expression was low in 34 (97%) tumors and elevated in one case (3%). MHC-I gene expression was upregulated in 10 (28.6%) tumors and 25 tumors (71.4%) revealed MHC-I gene downregulation. All patients received post-surgical radiotherapy. TMZ was given to 24 (68.6%) patients, while 11 (31.4%) patients received TMZ plus other adjuvant chemotherapies. The mean RFI was 16.7 months. All these results are presented in Table I.

Table II. The relationship between IDH mutation, MHC-I gene expression and CD8+ T-cell infiltration in tumor microenvironment

Parameter		CD8 T cell expression			
		High expression	Low expression	Total	*p*-value
IDH status	IDH-mutant	3 (42.9)	19 (67.9)	22 (62.9)	0.383[a]
	IDH-wildtype	4 (57.1)	9 (32.1)	13 (37.1)	
MHC-I expression	Downregulated	5 (71.4)	20 (71.4)	25 (71.4)	1.000[a]
	Upregulated	2 (28.6)	8 (28.6)	10 (28.6)	
IDH and MHC-I	IDH-mutant downregulated	2 (28.6)	14 (50.0)	16 (45.7)	0.565[a]
	IDH-wildtype downregulated	3 (42.9)	6 (21.4)	9 (25.7)	
	IDH-mutant upregulated	1 (14.3)	5 (17.9)	6 (17.1)	
	IDH-wildtype upregulated	1 (14.3)	3 (10.7)	4 (11.4)	

[a] *Significance values of Fisher's exact test*

Relationship between IDH mutation, MHC-I expression and CD8+ T-cell infiltration

Although CD8+ T-cells were found less infiltrated in IDH-mutant tumors, there was no statistically significant relationship between IDH mutation and CD8+ T-cell infiltration (p = 0.383) (Table II). There was also no statistically significant relationship between MHC-I expression, CD8+ T-cell infiltration and IDH mutation (p > 0.05). Nevertheless, IDH-mutant tumors with downregulated MHC-I had less cytotoxic T-cell infiltration.

Correlation of MHC-I, IDH mutation and CD8+ T-cell infiltration with RFI

Tumors with different levels of CD8+ T-cells and IDH mutational status exhibited a statistically significant difference in RFI (p = 0.012). IDH-wildtype tumors with highly infiltrated CD8+ T-cells or IDH-mutant tumors with low CD8+ T-cells showed late tumor recurrence (Fig. 3A).

The impact of TMZ and TMZ plus on RFI of tumors with different MHC-I expression levels and fluctuating degrees of CD8+ T-cells

We found a significant difference in RFI among tumors with varying levels of MHC-I expression in patients who received either TMZ alone or in combination with other chemotherapeutic agents (p = 0.026). Patients with downregulated MHC-I expression in their tumors who received TMZ plus showed a higher likelihood of experiencing late tumor recurrence compared to those who received only TMZ (Fig. 3B). We also found a statistically significant difference in RFI among tumors with varying degrees of CD8+ T-cell expression in patients who received either TMZ alone or TMZ plus (p = 0.023). Tumors with less infiltrated CD8+ T-cells who received TMZ plus had a late tumor recurrence compared to patients who received only TMZ (Fig. 3C). This indicates that the use of TMZ plus other chemotherapies had a more pronounced effect on tumor recurrence compared to using TMZ alone, regardless of CD8+ T-cell infiltration or MHC-I expression.

Discussion

MHC-I molecules play a crucial role in adaptive immunity by presenting their peptides to TILs. Once T-cells recognize these peptides, they initiate an immune response to eliminate the cells presenting the peptides. In the tumor microenvironment, the CD8 cytotoxic T-cell receptor interacts with each tumor cell that presents MHC-I peptides, leading to their destruction by the CD8 T-cell. This reciprocal communication is influenced by the capacity of CD8 T-cells to penetrate the tumor microenvironment, as well as the frequency of MHC-I peptides on the surface of tumor cells. However, our research found that this interplay between CD8+ T-cells and MHC-I peptides is not synergistic, as is typical in other contexts (Table II). The imbalance of either of these two elements can have an impact on the growth and progression of tumors. When MHC-I expression is downregulated, tumor cells may evade destruction by CD8+ T-cells, which become inactive as a result. In this case, regulatory T-cells (Tregs) inhibit the activity of CD8+ T-cells and prevent them from attacking tumor cells. Hence, tumor cells may grow and reproduce to a degree that makes them less responsive to treatment [18]. The presence of abundant CD8+ T-cells and MHC-I peptides in the tumor microenvironment has not been shown to be a key factor in preventing tumor progression.

The mechanism by which tumor cells downregulate the MHC-I gene and its presenting peptides to evade

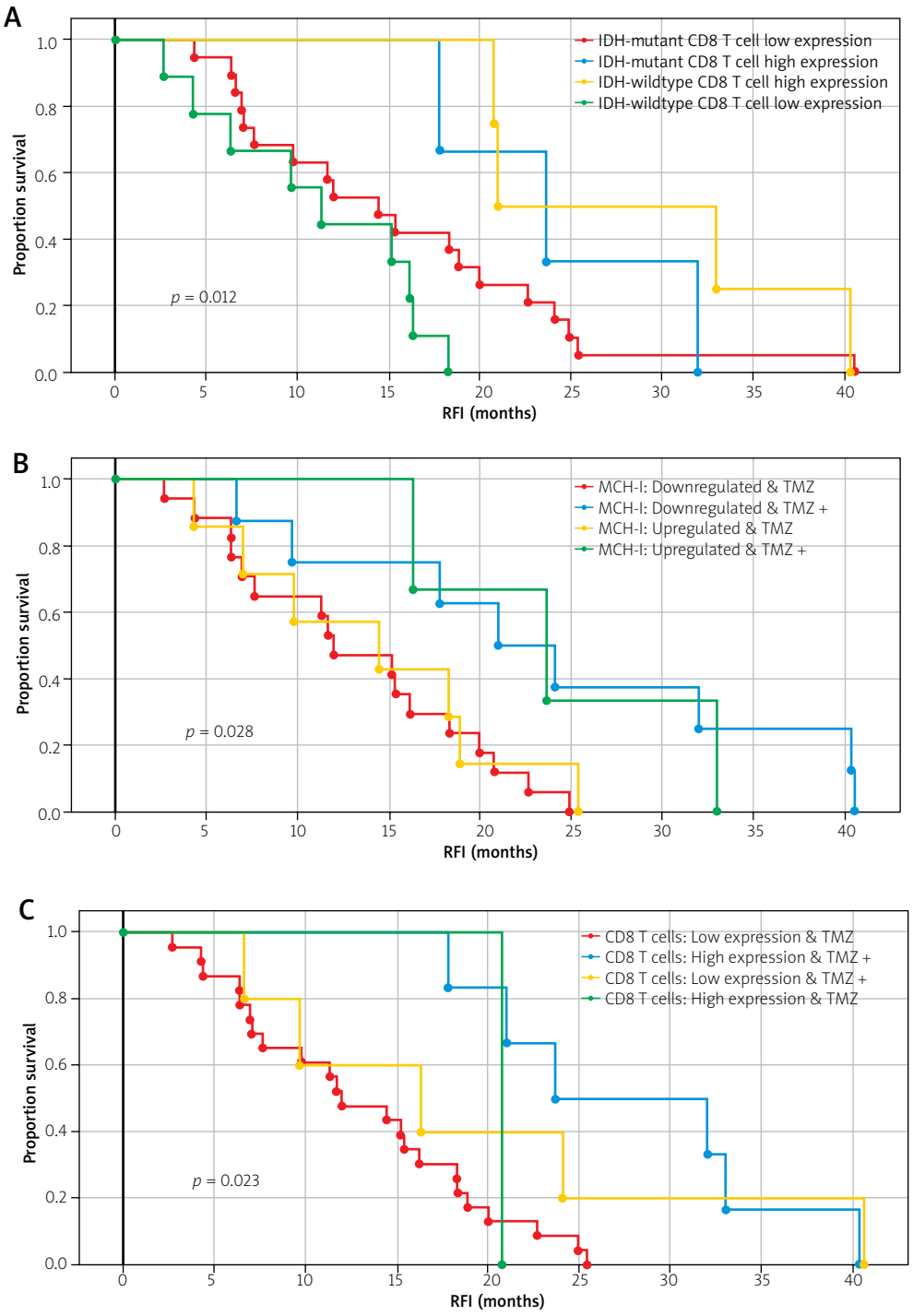

Fig. 3. The impact of TMZ and TMZ plus on the recurrence of WHO grade 4 astrocytoma in tumors exhibiting different MHC-I and CD8+ T-cell expression.

T-cells remains unclear, and several theories can be proposed to explain this process. Peptides presented by MHC-I are formed by proteasomal degradation of cytosolic proteins and are translocated into the endoplasmic reticulum by several receptors such as ERAP1 (endoplasmic reticulum aminopeptidase) and TAP1 (transporter associated with antigen processing 1) [2,8]. Castro *et al*. suggested that this transportation process

may be compromised by TP53 protein activation resulting in MHC-I downregulation [2]. It is important to note that not all mutations in TP53 lead to reduced expression of TAP1 and ERAP1, and the correlation between TP53 and these transporters may differ depending on the type of cancer and specific mutations present.

One potential mechanism responsible for MHC-I downregulation is the presence of TAMs. These TAMs may conceal the tumor cells, thereby hindering their identification by cytotoxic T-cells [10] (Fig. 1). TAMs may secrete some factors that block peptidase presentation on the MHC-I receptor. Moreover, tumor cells can downregulate MHC-I expression as a mechanism of immune evasion. This might occur as a result of modifications in the expression of transcription factors that control MHC-I regulation, as well as abnormalities in signaling pathways that oversee its expression. Another factor that can also contribute to MHC-I downregulation in the tumor microenvironment is the presence of regulatory T cells (Tregs). Tregs can suppress the activity of MHC-I presentation and recognition [18].

Downregulated MHC-I might be enhanced by chemotherapies. TMZ is a standard treatment for WHO grade 4 astrocytoma, and it has been shown to have an impact on the immune system [25]. In a study performed by Zhang *et al*., on glioblastoma stem cells (GSCs), TMZ enhanced MHC-I expression, and NF-κB was activated. TMZ treatment increased MHC-I expression *via* modulation of NF-κB signaling in GSCs. Apart from its role as a chemotherapeutic agent, TMZ can also act as an immunomodulatory agent when used for treating patients with glioma [27]. Until now, no research investigating the association between MHC-I expression or CD8 cytotoxic T-cell infiltration and the use of TMZ in combination with other chemotherapeutic agents has been conducted. However, studies have demonstrated that the use of adjuvant therapies along with TMZ results in superior outcomes in terms of tumor recurrence. Our findings indicate that the use of TMZ in combination with other adjuvants resulted in improved patient survival and delayed tumor recurrence, as compared to patients who were solely treated with TMZ (Fig. 3B). One possible explanation for this could be that adjuvant chemotherapies, which are not TMZ-based, may have a greater ability to sensitize tumors to cytotoxic T-cells compared to TMZ alone. This finding suggests that adding adjuvant chemotherapies to the treatment protocol for glioma, particularly in cases of non-MGMT methylated tumors, could be beneficial and should be considered by oncologists as a routine practice.

The association between IDH mutation and CD8 cytotoxic T-cells in the microenvironment of high-grade glioma has never been thoroughly investigated. We found no relationship between IDH mutation and $CD8^+$ T-cell expression in the tumor microenvironment. The impact was only noticeable when both parameters were compared to RFI. IDH-wildtype tumors with highly infiltrated $CD8^+$ T-cells or IDH-mutant tumors with low $CD8^+$ T-cells showed late tumor recurrence (Fig. 3A). This indicates that no association between IDH mutations and $CD8^+$ T-cells has been scientifically demonstrated. IDH is directly associated with tumor recurrence, irrespective of the density of CD8 cytotoxic T-cell infiltration.

Conclusions

Our study found no scientific evidence linking IDH mutation with infiltrated cytotoxic T-cells in the microenvironment of WHO grade 4 astrocytoma. Nonetheless, IDH is directly linked to tumor recurrence. The combined use of TMZ with other adjuvants has been proven to be more effective in improving patient survival and delaying tumor recurrence, as compared to using TMZ alone. Hence, non-TMZ adjuvant chemotherapies may be more effective in sensitizing tumors to cytotoxic T-cells than TMZ.

Acknowledgments

Special thanks to the Deanship of Scientific Research at King Abdulaziz University for support.

Disclosure

The authors report no conflict of interest.

References

1. Castro F, Cardoso AP, Goncalves RM, Serre K, Oliveira MJ. Interferon-gamma at the crossroads of tumor immune surveillance or evasion. Front Immunol 2018; 9: 847.
2. Castro M, Sipos B, Pieper M, Biskup S. Major histocompatibility complex [MHC1] loss among patients with glioblastoma. JCOC 2020; 38.
3. Chen DS, Mellman I. Elements of cancer immunity and the cancer-immune set point. Nature 2017; 541: 321-330.
4. Chen Z, Hambardzumyan D. Immune microenvironment in glioblastoma subtypes. Front Immunol 2018; 9: 1004.
5. Feng L, Qian H, Yu X, Liu K, Xiao T, Zhang C, Kuang M, Cheng S, Li X, Wan J, Zhang K. Heterogeneity of tumorinfiltrating lymphocytes ascribed to local immune status rather than neoantigens by multi-omics analysis of glioblastoma multiforme. Sci Rep 2017; 7: 6968.
6. Gerloni M, Zanetti M. CD4 T cells in tumor immunity. Springer Semin Immunopathol 2005; 27: 37-48.
7. Han S, Zhang C, Li Q, Dong J, Liu Y, Huang Y, Jiang T, Wu A. Tumour-infiltrating CD4+ and CD8+ lymphocytes as predictors of clinical outcome in glioma. Br J Cancer 2014; 110: 2560-2568.
8. Kilian M, Sheinin R, Tan CL, Friedrich M, Krämer C, Kaminitz A, Sanghvi K, Lindner K, Chih YC, Cichon F, Richter B, Jung S, Jähne K, Ratliff M, Prins RM, Etminan N, von Deimling A, Wick W, Madi A, Bunse L, Platten M. MHC class II-restricted antigen presentation is required to prevent dysfunction of cytotoxic T cells by

blood-borne myeloids in brain tumors. Cancer Cell 2023; 41: 235-251.e9.
9. Kmiecik J, Poli A, Brons NH, Waha A, Eide GE, Enger PØ, Zimmer J, Chekenya M. Elevated CD3+ and CD8+ tumorinfiltrating immune cells correlate with prolonged survival in glioblastoma patients despite integrated immunosuppressive mechanisms in the tumor microenvironment and at the systemic level. J Neuroimmunol 2013; 264: 71-83.
10. Kurdi M, Alghamdi B, Butt NS, Baeesa S. The relationship between CD204 ^{M2}-polarized tumour-associated macrophages [TAMs], tumour-infiltrating lymphocytes [TILs], and microglial activation in glioblastoma microenvironment: a novel immune checkpoint receptor target. Discov Oncol 2021; 25: 28.
11. Largeot A, Pagano G, Gonder S, Moussay E, Paggetti J. The B-side of cancer immunity: The underrated tune. Cells 2019: 8: 449.
12. Louis DN, Perry A, Wesseling P, Brat DJ, Cree IA, Figarella-Branger D, Hawkins C, Ng HK, Pfister SM, Reifenberger G, Soffietti R, von Deimling A, Ellison DW. The 2021 WHO Classification of Tumors of the Central Nervous System: a summary. Neuro Oncol 2021; 23: 1231-1251.
13. Nazemalhosseini-Mojarad E, Mohammadpour S, Torshizi Esafahani A, Gharib E, Larki P, Moradi A, Porhoseingholi MA, Asadzade Aghdaei H, Kuppen PJK, Reza Zali M. Intratumoral infiltrating lymphocytes correlate with improved survival in colorectal cancer patients: Independent of oncogenetic features. J Cell Physiol 2019; 234: 4768-4777.
14. Nimmerjahn A, Kirchhoff F, Helmchen F. Resting microglial cells are highly dynamic surveillants of brain parenchyma in vivo. Science 2005; 308: 1314-1318.
15. Parajuli P, Mittal S. Role of IL-17 in glioma progression. J Spine Neurosurg 2013; Suppl 1: S1-004.
16. Philip M, Fairchild L, Sun L, Horste EL, Camara S, Shakiba M, Scott AC, Viale A, Lauer P, Merghoub T, Hellmann MD, Wolchok JD, Leslie CS, Schietinger A. Chromatin states define tumour-specific T cell dysfunction and reprogramming. Nature 2017; 545: 452-456.
17. Philip M, Schietinger A. CD8+ T cell differentiation and dysfunction in cancer. Nat Rev Immunol 2022; 22: 209-223.
18. Quezada SA, Peggs KS, Simpson TR, Allison JP. Shifting the equilibrium in cancer immunoediting: from tumor tolerance to eradication. Immunol Rev 2011; 241: 104-118.
19. Quail DF, Joyce JA. The microenvironmental landscape of brain tumors. Cancer Cell 2017; 31: 326-341.
20. Lam H, McNeil LK, Starobinets H, DeVault VL, Cohen RB, Twardowski P, Johnson ML, Gillison ML, Stein MN, Vaishampayan UN, DeCillis AP, Foti JJ, Vemulapalli V, Tjon E, Ferber K, DeOliveira DB, Broom W, Agnihotri P, Jaffee EM, Wong KK, Drake CG, Carroll PM, Davis TA, Flechtner JB. An empirical antigen selection method identifies neoantigens that either elicit broad antitumor T-cell responses or drive tumor growth. Cancer Discov 2021; 11: 696-713.
21. St Paul M, Ohashi PS. The roles of CD8+ T cell subsets in antitumor immunity. Trends Cell Biol 2020; 30: 695-704.
22. Stupp R, Mason WP, van den Bent MJ, Weller M, Fisher B, Taphoorn MJ, Belanger K, Brandes AA, Marosi C, Bogdahn U, Curschmann J, Janzer RC, Ludwin SK, Gorlia T, Allgeier A, Lacombe D, Cairncross JG, Eisenhauer E, Mirimanoff RO; European Organisation for Research and Treatment of Cancer Brain Tumor and Radiotherapy Groups; National Cancer Institute of Canada Clinical Trials Group. Radiotherapy plus concomitant and adjuvant TMZ for glioblastoma. N Engl J Med 2005; 352: 987-996.
23. Liu S, Yang Z, Li G, Li C, Luo Y, Gong Q, Wu X, Li T, Zhang Z, Xing B, Xu X, Lu X. Multi-omics analysis of primary cell culture models reveals genetic and epigenetic basis of intratumoral phenotypic diversity. Genomics Proteomics Bioinformatics 2019; 17: 576-589.
24. Thommen DS, Schumacher TN. T cell dysfunction in cancer. Cancer Cell 2018; 33: 547-562.
25. Weiss T, Weller M, Roth P. Immunotherapy for glioblastoma: concepts and challenges. Curr Opin Neurol 2015; 28: 639-646.
26. Wherry EJ, Kurachi M. Molecular and cellular insights into T cell exhaustion. Nat Rev Immunol 2015; 15: 486-499.
27. Zhang D, Qiu B, Wang Y, Guan Y, Zhang L, Wu A. Temozolomide increases MHC-I expression via NF-‑B signaling in glioma stem cells. Cell Biol Int 2017; 41: 680-690.